Adsorption (2006) 12:205–212
DOI 10.1007/s10450-006-0146-z

Adsorption of acrylonitrile and methyl acrylate on activated carbon in a packed bed column

Fengsong Wang · Jun Li · Jiarong Wang · Haoqi Gao

Received: 28 March 2006 / Revised: 6 July 2006 / Accepted: 5 September 2006
© Springer Science + Business Media, LLC 2006

Abstract The adsorption equilibrium and dynamics of acrylonitrile (ACN), methyl acrylate (MA) and the ACN-MA mixture on activated carbon were investigated in a packed bed column at 40°C. The study indicated that the adsorption isotherms of the pure components belong to the classical Langmuir type; in the case of the binary mixture adsorption, the Ideal Adsorption Solution Theory (IAST) could predict better than the Extended Langmuir (E-L) equation in particular for the MA component. The mass balance equations were established to describe the adsorption dynamic behaviors of the gas phase in the packed bed column, and the linear driving force (LDF) approximation was adopted to estimate the absorbate adsorption kinetics onto the adsorbent. The coupled partial differential equations of the model were numerically solved by the orthogonal collocation (OC) method. The correlated results showed that the model could give an acceptable description of the breakthough curves of the pure ACN and MA in the packed bed column. The prediction of the breakthough curves for the binary CAN-MA system at different inlet concentrations was also implemented, indicating a good agreement with the experimental data.

Keywords Adsorption equilibrium · Dynamics · Acrylonitrile · Methyl acrylate · Packed bed column

F. Wang · J. Li (✉)
Department of Chemical Engineering and Biochemical Engineering, Xiamen University, Xiamen 361005, China
e-mail: junnyxm@xmu.edu.cn

J. Wang · H. Gao
Department of Chemical Engineering, Ningbo University of Science and Technology, Ningbo 315016, China

1 Introduction

In manufacturing acrylic fibers, volatile organic compounds (VOCs) mainly including acrylonitrile (ACN) and methyl acrylate (MA) are produced. ACN, a highly toxic VOC and carcinogen with boiling point 77.3°C, makes people feel sick, vomit when they inhale even very small quantity. MA with boiling point 80.3°C may hurt human's lung, liver or kidney through skin contact for a long time. Therefore the exhaust of those VOCs should be strictly controlled; for example, the limitation of the ACN emission in a waste gas according to the national standard (GB16297, 1996) is less than 26 mg/m^3.

VOCs can be treated with many methods (Moretti and Mukhopadhyay, 1993); they can be classified as the following two types: one is the destroying approach (such as burning or biological method) to transform the VOCs into nontoxic substances; the other includes adsorption, sorption, membrane separation, etc. to recover the VOCs from waste gases. In the latter one the adsorption method has been widely studied, where active carbon is commonly used as the

adsorbent in the process due to its high specific surface, adsorption capacity, easy recovery and abundant resources.

Adsorption equilibrium data and adsorption dynamics are the fundamental knowledge of the adsorption technology and equipment design. This work studies experimentally and theoretically the adsorption behaviors (adsorption equilibrium and adsorption dynamics) of the pure ACN, the pure MA and the ACN-MA mixture onto active carbon in a packed bed column.

2 Experimental

To measure the equilibrium data of a gas/vapor onto an absorbent, two methods are commonly used: the static method and the dynamic method (Yun et al., 1999). The later one measures the adsorbate concentration in the exit gas of an adsorption column, and the equilibrium data and dynamic data can be obtained simultaneously; using gravimetric analysis of the adsorbent, it can also provide the equilibrium data of pure substances; and furthermore this method ensures a quick equilibrium between the adsorbent (solid) phase and the gas phase. In this work we adopted the dynamic method with a packed bed column.

2.1 Materials

The granular active carbon provided by Shanghai Active Carbon Factory has the properties listed in Table 1. It was pretreated under 160°C more than 2 h before use. Acrylonitrile and methyl acrylate were purchased from Shanghai Chemical Reagent Company with AP grade without further purification.

Table 1 Properties of active carbon

Properties	Values
Average diameter (mm)	1.5
Particle density (kg/m^3)	750
Bulk density (kg/m^3)	550
Particle porosity	0.40
Bed void fraction	0.27

2.2 Apparatus and method

The experimental apparatus is composed of two units as shown in Fig. 1: gas preparation and adsorption.

In the gas preparation unit, the pure and dried carrier gas N_2 is divided into two branches: one bubbles through the desired solution in the liquid vessel (ACN or MA or their mixture) at ambient temperature, and then the volatile absorbates are transferred from the matrix into the gas phase; the other directly goes into the mixture vessel to form the desired concentration of the feed gas. The adsorption unit consists of a thermostat and an adsorption column (Ø15(ID) × 200 mm) with a jacket for controlling temperature (with uncertainty of ±0.1°C) by circulating heated water. The inlet gas from the mixture vessel is preheated and mixed in a coil tube installed before the adsorption column. The concentration of the exit absorbate from the adsorption column was measured by a gas chromatography (GC-14B) using the flame ionization detector (FID). The GC column is a stainless steel tube (Ø3 × 2000 mm) packed with GDX–103 (60–80 mesh), the hydrogen flow rate

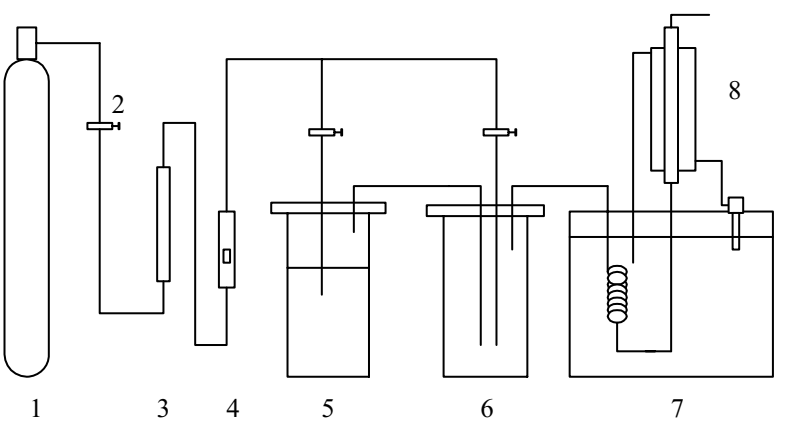

Fig. 1 Schematic experimental equipment. (1) N_2 bottle; (2) valve; (3) drier; (4) flow meter; (5) liquid vessel; (6) gas mixture vessel; (7) thermostat; (8) adsorption column

is 50 mL/min, 5 mL sample is used, the GC column temperature is 210°C, the injection port temperature is 250°C and the detector temperature is 200°C. Throughout the experiment, it was maintained at atmospheric pressure.

The concentration of absorbate (ACN or MA) in the exit gas of the adsorption column was analyzed by comparing measured peak areas to the standard curves. To obtain the standard curves, ACN was dissolved into CCl_4 to prepare solutions with five different concentrations to obtain different peak areas by the GC analysis. The same procedure was implemented for MA which was dissolved into CS_2 for preparing the standard solutions.

For the pure compounds, the change of the mass of absorbent before and after adsorption can directly provide the adsorption equilibrium data. For the binary system, the breakthrough curves ought to be used to obtain the adsorption equilibrium data for each component. In the adsorption process, the flow rate of carrier gas N_2 and the operation temperature are constants; therefore the following formula is used for calculating the equilibrium data through the breakthrough curves:

$$q_{e_i} = \frac{M_i F}{w}\left(C_{io}t_s - \int_0^{t_s} C_i dt\right) \times 10^{-6} \qquad (1)$$

where q_{ei} is the mass of species i adsorbed in the adsorbent, F is the volume flow rate of gas phase (32 L/min), w is the mass of the loaded adsorbent (about 25 g active carbon) in the column, C_{i0} is the inlet concentration of compound i, t_s is the saturation time of the adsorbent, C_i is the exit concentration of compound i at time t, M_i is the molecular weight of compound i. To obtain q_{ei} accurately and conveniently, a program was coded with the Spline interpolation algorithm utilizing the scattered experimental data to solve the integral of Eq. (1). The accordance between the gravimetric results and the results from Eq. (1) is acceptable for the pure ACN and the pure MA (with a maximum difference about 5 mg/g).

3 Adsorption equilibrium

3.1 Adsorption equilibrium data

The measured adsorption equilibrium data of the pure ACN and MA obtained from Eq. (1) at 40°C are shown in Fig. 2. It indicates that the active carbon used in this study has a higher adsorption capacity for MA than that for ACN. The binary equilibrium data obtained from Eq. (1) with the binary breakthrough data were shown in Fig. 3.

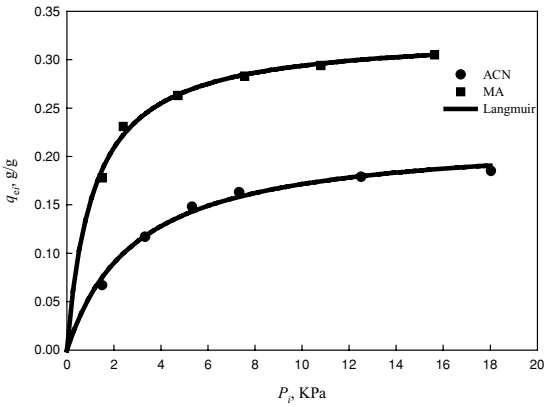

Fig. 2 Correlated and experimental adsorption isotherms of ACN and MA at 40°C. Points: experimental; lines: correlated

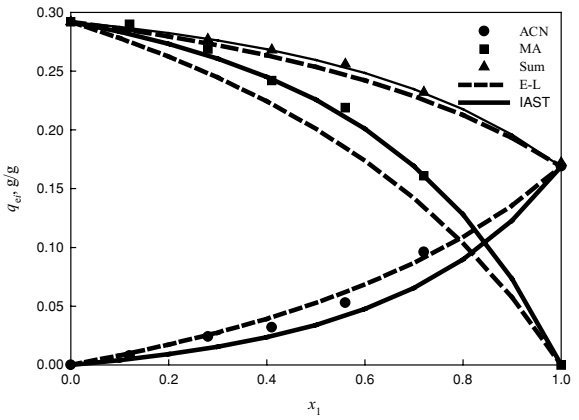

Fig. 3 Predicted and experimental adsorption isotherms of the binary ACN-MA mixture at 40°C. Points: experimental; lines: predicted

3.2 Correlation and prediction of the adsorption isotherms

The adsorption of organic vapors onto active carbon usually belongs to the type I isotherm, which can be described by the classic Langmuir equation

$$q_{ei} = \frac{q_{\max i} K_i p_i}{1 + K_i p_i} \quad i = 1, 2 \qquad (2)$$

Table 2 Langmuir adsorption constants at 40°C

Compounds	$q_{\max i}$ (g/g)	K_i (1/KPa)	K_i (m^3/kg)
ACN	0.2218	0.3399	16. 68
MA	0.3271	0.8783	26.56

where, $q_{\max i}$ represents the maximum adsorption capacity, K_i is the Langmuir constant, p_i is the vapor fraction pressure of species i in the gas mixture. Subscript $i = 1$ denotes ACN and $i = 2$ represents MA. Using Eq. (2), the experimental adsorption isotherms of ACN and MA were correlated and indicated in Fig. 2. The correlation shows the Langmuir equation is obviously suitable for the studied systems; the correlated Langmuir constants are illustrated in Table 2, in which two sets of K_i were presented in order to conveniently apply them to different cases. K_i in m^3/kg will be used in dynamic modeling (Eqs. (17) and (18)) in the case of the Langmuir equation; and K_i in (1/kPa) will be applied to Eqs. (A2), (A4) and (19) in the case of the IAST equations.

For the binary ACN-MA system, the adsorption isotherms can be predicted with above correlation information of the pure compounds. The extended Langmuir (E-L) equation is widely used due to its simplicity, and can be expressed as

$$\frac{q_{ei}}{q_{\max i}} = \frac{K_i p_i}{1 + K_1 p_1 + K_2 p_2} \quad i = 1, 2 \tag{3}$$

where we can directly use the Langmuir constants listed in Table 2. The predicted results are shown in Fig. 3 with the abscissa x_i ($i = 1$) being the ACN molar fraction in the inlet gas mixture of the adsorption column in the absence of the carrier gas N_2 and has the following relationship with p_i

$$x_i = \frac{C_{i0}}{C_{10} + C_{20}} = \frac{p_i}{p_1 + p_2} \quad i = 1, 2 \tag{4}$$

The experimental points at $x_1 = 1$ and $x_1 = 0$ in Fig. 3 were interpolated from the data shown in Fig. 2 for the pure compounds.

We also tested the Ideal Adsorption Solution Theory (IAST) (Myers and Prausnitz, 1965) to predict the binary adsorption equilibrium. As shown in Fig. 3, the IAST predicts much better for the MA component than the E-L equation does; on the contrary, the E-L equation predicts slightly better than the IAST does for ACN. The corresponding IAST formulae are presented in the Appendix. Figure 3 also shows the comparison of the experimental and the predicted adsorption isotherms of the ACN-MA mixture, it indicates that the IAST gives a better prediction.

4 Adsorption dynamics

4.1 Model

As mentioned, using the dynamic method we can obtain simultaneously the adsorption equilibrium data and the adsorption dynamic data from the packed bed column as shown in Figs. 4–6. Modeling those breakthrough curves is important for designing an adsorption column. For the adsorption process studied here, the energy and moment balance calculations are not required; we need only the mass balance equation, in

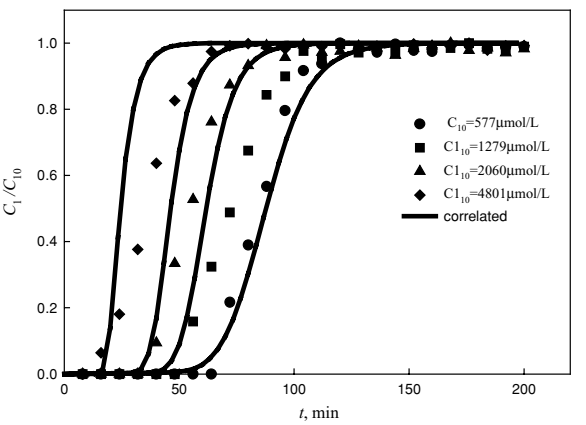

Fig. 4 Breakthrough curves of ACN at different inlet concentrations. Points: experimental; lines: correlated

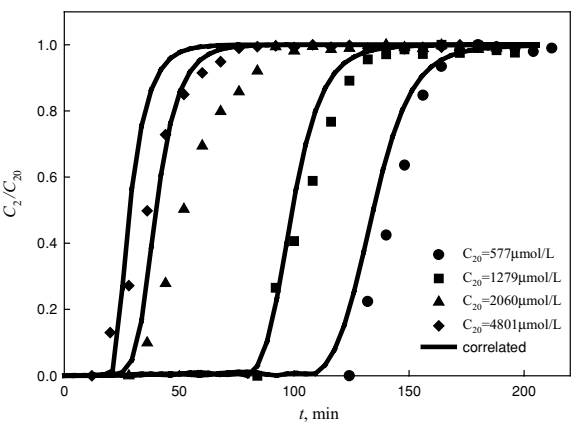

Fig. 5 Breakthrough curves of MA at different inlet concentrations. Points: experimental; lines: correlated

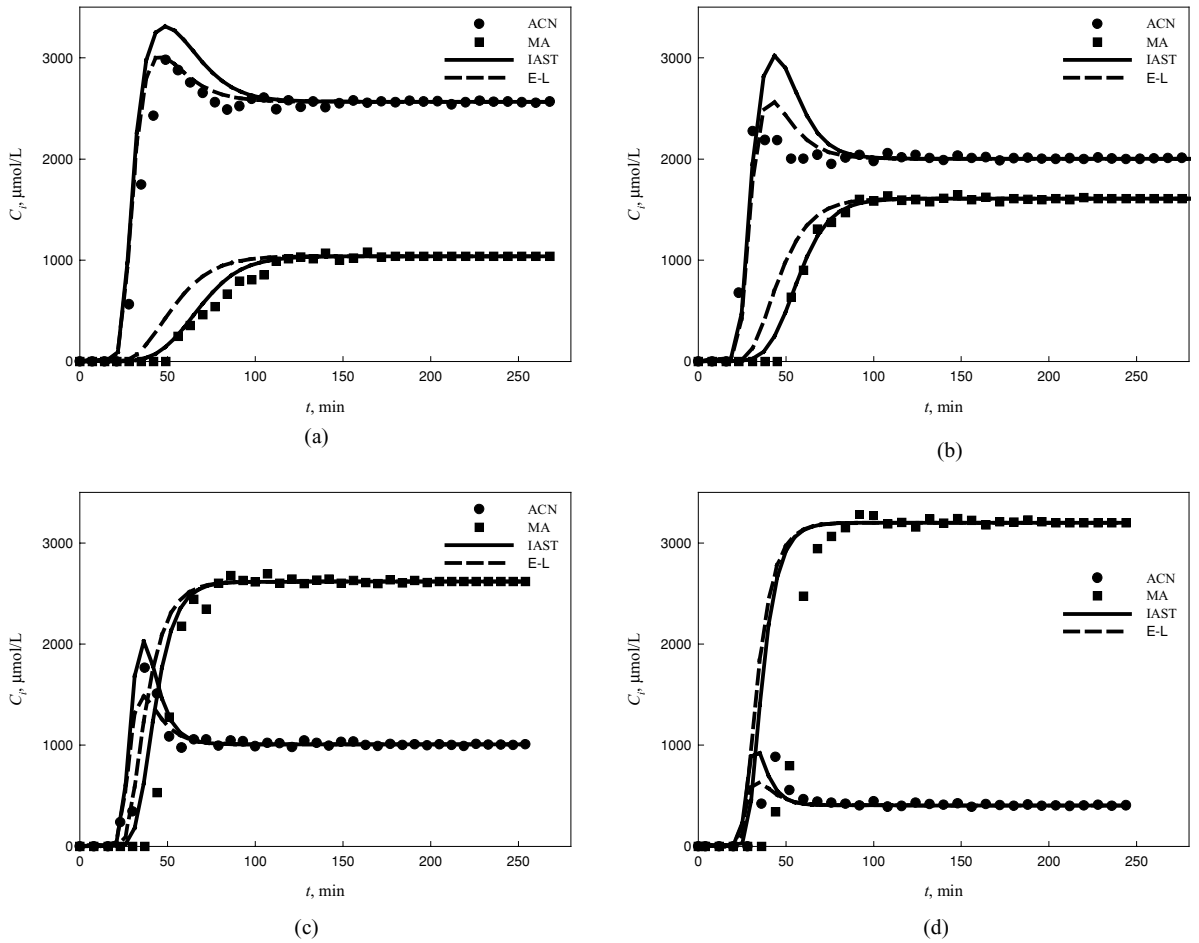

Fig. 6 Breakthrough curves of the ACN-MA system at different inlet concentrations. Inlet molar fraction of ACN (x_1): (a) 0.72; (b) 0.56; (c) 0.41; (d) 0.28. Points: experimental; lines: predicted

which the information of adsorption equilibrium and mass transfer between the gas phase and the solid phase is necessary.

In order to simplify the modeling, following reasonable assumptions are made: (1) ACN or MA or their mixture is dilute in the carrier gas; (2) active carbon particles are spherical, and the equilibrium is achieved on their outer surface; (3) the gas phase is continuous; (4) the axial diffusion is neglected for a small column. Therefore, with above simplifications we have the mass balance equation for component i in a packed bed column

$$v\frac{\partial c_i}{\partial z} + \frac{\partial c_i}{\partial t} + \frac{1-\varepsilon_B}{\varepsilon_B}\rho_P \frac{\partial \overline{q_i}}{\partial t} = 0 \tag{5}$$

where c_i is the absorbate concentration in the gas phase at position z of the adsorption column and at time t, v is the interstitial velocity of the gas, ε_B is the bed void fraction, ρ_P is the bulk density of active carbon, and $\overline{q}_i$ a volume-average concentration in the solid phase can be expressed as

$$\overline{q_i} = \frac{3}{R^3}\int_0^R q_i r^2 dr \tag{6}$$

where, R is the average radius of the active carbon particles, q_i is the absorbate concentration in the solid phase at t and r (radial position along the core of the active carbon particle).

The boundary and initial conditions of Eq. (5) are

$$c_i(0,t) = C_{i0}, \quad \left[\frac{\partial c_i}{\partial z}\right]_{z=L} = 0 \tag{7}$$

$$c_i(Z,0) = 0, \quad q_i(Z,r,0) = 0 \tag{8}$$

where C_{i0} is the inlet absorbate concentration at $z = 0$ in the gas phase (the same as that in Eq. (1)), L is the length of the adsorption column. In Eq. (5), we need to express the mass transfer equation between the continuous gas phase and the adsorbent solid phase. Although many studies were reported on this issue (Mendes et al., 1995; Do and Mayfield, 1987; Lai and Tan, 1991; Buaznowski and Yang, 1989), the linear driving force (LDF) approximation still has its potential utilization due to its simplicity. The LDF for a compound i can be expressed as

$$\frac{\partial \overline{q}_i}{\partial t} = k_i a_i (q_{ei} - \overline{q}_i) \tag{9}$$

with the initial condition

$$\overline{q}_i(0) = 0 \tag{10}$$

where $k_i a_i$ is the area-mass transfer coefficient of component i on the solid particle surface. It is Eq. (9) that connects to the adsorption equilibrium data. For the pure compounds, the Langmuir equation is used and the area-mass transfer coefficient at different conditions is correlated with experimental breakthrough curves. For the binary system, both the E-L equation and the IAST equations can be applied to the predictions with the information from the pure compounds.

4.2 Numerical solutions

Many numerical methods can be employed to solve above partial differential equations (PDE) for instance, method of line (MOL) and finite difference method. Here we used the orthogonal collocation (OC) method (Villadsen and Stewart, 1967) because it has some advantages over other methods, such as not many collocation points, and simple preparation before calculation. Using the OC method, we need to define following non-dimensional variables to simplify above model equations:

$$X_i = \frac{c_i}{C_{i_0}}, \quad Y_i = \frac{q_i}{q_{\max i}}, \quad Z = \frac{z}{L}, \quad T = \frac{v}{L} \cdot t,$$
$$\delta_i = \frac{\rho_P q_{\max i}}{\alpha C_{i_0}}, \quad \alpha = \frac{\varepsilon}{1-\varepsilon}, \quad \theta_i = \frac{k_i a_i L}{v},$$
$$K_{ci} = K_i C_{i_0} \tag{11}$$

In Eq. (11) some variable units should be emphasized: c_i and ρ_P are in kg/m^3 (in the calculation, c_{i0} should be changed from the original μmol/L to kg/m^3 at 40°C using the ideal gas equation of state); L and z are in m, v in m/min obtained from the flow rate F and the adsorption column diameter. So, $k_i a_i$ is in 1/min and K_i is in m^3/kg as listed in Table 2. To avoid any misunderstanding, we also note that $C_i = c_i\,(z = L, t)$ which is needed in a breakthrough curve. Therefore, Eqs. (5), (7) and (8–10) are transformed respectively to

$$\frac{\partial X_i}{\partial Z} + \frac{\partial X_i}{\partial T} + \delta_i \frac{\partial \overline{Y}_i}{\partial T} = 0 \quad i = 1, 2 \tag{12}$$

$$X_i(0, T) = 1, \quad \left[\frac{\partial X_i}{\partial Z}\right]_{Z=1} = 0 \tag{13}$$

$$X_i(Z, 0) = 0, \quad \overline{Y}_i(Z, 0) = 0 \tag{14}$$

$$\frac{\partial \overline{Y}_i}{\partial T} = \theta_i (Y_{ei} - \overline{Y}_i) \quad i = 1, 2 \tag{15}$$

$$\overline{Y}_i(0) = 0 \tag{16}$$

And the adsorption equilibrium equations expressed with the Langmuir equation for the pure compounds and for the binary system are respectively

$$Y_{ei} = \frac{K_{ci} X_i}{1 + K_{ci} X_i} \tag{17}$$

$$Y_{ei} = \frac{K_{ci} X_i}{1 + K_{c1} X_1 + K_{c2} X_2} \tag{18}$$

When the IAST equations are used for the binary system, it can be written as

$$Y_{ei} = \frac{x_i q_t}{q_{\max i}} = \frac{x_i}{q_{\max i}} \left(\frac{1}{a_1 + a_2}\right),$$
$$a_i = \frac{x_i \left(1 + K_i p_i^0\right)}{q_{\max i} K_i p_i^0} \quad i = 1, 2 \tag{19}$$

All those new variables used in Eq. (19) are defined in the Appendix, and K_i ought to be in (1/kPa) in Eq. (19).

Then Eqs. (12) and (15) can be separated into discrete equations by the OC method in the Z-direction; the Legendre polynomials with 6 degrees (its 6 real roots are the interior collocation points) were applied in the OC method. Our modeling showed that the result with 6 interior collocation points is very close to that

with 8 interior collocation points; in this regard, the calculations were carried out with 6 interior collocation points for all cases in this work. With above transformation, Eqs. (12) and (15) are now ordinary differential equations with respect to T and could be easily solved.

4.3 Correlations for the pure compounds

The correlation results for the pure ACN and MA are shown in Figs. 4 and 5 separately. The figures indicate the correlation is acceptable although the agreement is not very good at higher inlet concentrations. This correlation also showed that the breakthrough curves are very sensitive to $q_{\max i}$, much more sensitive than K_i. A slight change of $q_{\max i}$ will obviously vary the correlated breakthrough curves. For example, when $q_{\max i}$ times 1.1 the breakthrough time at the inlet concentration 577 μmol/L for MA will shift from about 110 min to more than 130 min, highly postponing the breakthrough curves. Therefore an accurate measurement of the equilibrium data, in particular the breakthrough time, is crucial to give an accurate description of the adsorption dynamics by modeling. We through the correlations obtained the average $k_i a_i = 0.0037$ (1/min) for ACN and $k_i a_i = 0.0027$ (1/min) for MA. This area-mass transfer coefficient plays an important role on the slopes of the breakthrough curves, and we did not find evident concentration dependence of this parameter; but from those experimental points as shown in Figs. 4 and 5, it may suggest that a higher inlet concentration corresponds to a lower $k_i a_i$ value.

4.4 Predictions for the binary system

The predicted results for the binary ACN-MA system with the E-L equation or the IAST equations to describe the adsorption dynamics are shown in Fig. 6. It is indicated the model with the IAST equations can give a good description of the binary system's breakthrough curves and give a larger saturation time for all the studied cases, indicating a slightly better agreement with the experimental breakthrough curves for the MA compound; but the IAST predicts a slightly worse result of the maximum adsorption capacity of ACN than the E-L equation. This is accordant to the prediction of the adsorption isotherms, in which the IAST gives relatively better adsorption isotherms of MA while the E-L equation gives a relatively better adsorption description of ACN.

5 Conclusions

This work studied experimentally and theoretically the adsorption equilibrium and dynamics of CAN, MA, and their mixture on active carbon in a packed bed column. Through this investigation, we have following conclusions:

(1) The active carbon used here has high adsorption capacities for ACN and MA; the adsorbed capacity reaches 221.8 mg/g and 327.1 mg/g at 40°C for ACN and MA, respectively.
(2) The adsorption equilibrium isotherms of the pure ACN and MA are typical Langmuir type, so the Langmuir equation can be employed to the experimental data correlations. The E-L equation and the IAST equations can be used to predict the binary system's adsorption isotherms; this prediction shows that the IAST equations are better than the E-L equation to describe the studied binary system in particular for the MA component.
(3) The mass balance equation to model the breakthrough curves of the studied system, resolved by the orthogonal collocation (OC) method showed that it could give prediction results in a good agreement with the experimental data including both the IAST and the E-L equation. The IAST predicts a slightly better breakthrough data of the MA compound, but a slightly worse result of the maximum adsorption capacity of the ACN compound than the E-L equation does.

Nomenclature

C_{i0}	inlet concentration of compound i, μmol/L
C_i	outlet concentration of compound i at time t, μmol/L
c_i	absorbate concentration in gas phase at position z and at time t, μmol/L
F	volume flow rate of gas phase, L/min
K_i	Langmuir constants of species i, 1/KPa, or m^3/kg
$k_i a_i$	area-mass transfer coefficient of component i, 1/min
L	length of adsorption column, m
M_i	molecular weight of compound i, g/mol
p_i	vapor fraction pressure of species i, Kpa
q_{ei}	mass of species i adsorbed, g/g

$q_{\max i}$	maximum adsorption capacity, g/g
$\overline{q}_i$	volume-average concentration in solid phase, g/g
q_i	absorbate concentration in solid phase at t and r (radial position), g/g
R	average radius of active carbon particles, m
t_s	saturation time, min
v	interstitial velocity of carrier gas, m/s
w	mass of loaded adsorbent, g
ε_B	bed void fraction
ρ_P	bulk density of active carbon, m^3/kg

Appendix: Calculation formulae of the IAST

The species adsorption at equilibrium can be calculated as

$$q_{ei} = x_{si}\, q_t \tag{A1}$$

where x_{si} is the absorbate molar fraction in solid phase. The total adsorption capacity q_t is expressed

$$\frac{1}{q_t} = \frac{x_{s1}\left(1 + K_1 p_1^0\right)}{q_{\max 1} K_1 p_1^0} + \frac{x_{s2}\left(1 + K_2 p_2^0\right)}{q_{\max 2} K_2 p_2^0} \tag{A2}$$

with

$$p y_{gi} = x_{si}\, p_i^0 \ (i = 1, 2) \tag{A3}$$

$$\left(1 + K_1 p_1^0\right)^{q_{\max 1}} = \left(1 + K_2 p_2^0\right)^{q_{\max 2}} \tag{A4}$$

where y_{gi} is the molar fraction of component$i$ in gas phase which is obtained from C_i in the text, p_i^0 is defined as the gas pressure when only component i is present. (A3)–(A4) should be solved to obtain x_{si} and p_i^0 in order to obtain q_t.

Acknowledgment The support from Zhejiang Jinyong Acrylic Fiber Company for carrying out this study is gratefully acknowledged.

References

Buaznowski, M.A. and R.T. Yang, "Extended Linear Driving Force Approximation for Intraparticle Diffusion Rate Including Short Times," *Chem. Eng. Sci.*, **44**, 2683–2689 (1989).

Do, D.D. and P.L.J. Mayfield, "A New Simplified Model for Adsorption in a Single Particle," *AIChE J.*, **33**, 1397–1400 (1987).

Lai, C.C. and C.S. Tan, "Approximate Models for Nonlinear Adsorption in a Packed-Bed Adsorber," *AIChE J.*, **37**, 461–465 (1991).

Moretti, E.C. and N. Mukhopadhyay, "VOCS Control Current Practices and Future Trends," *Chem. Eng. Prog.*, **6**, 20–26 (1993).

Myers, A.L. and J.M. Prausnitz, "Thermodynamics of Mixed-Gas Adsorption," *AIChE J.,* **11**, 121–127 (1965).

Mendes, A.M.M., C.A.V. Costa, and A.E. Rodrigues, "Linear Driving Force Approximation for Isothermal Non-Isobaric Diffusion/Convection with Binary Langmuir Adsorption," *Gas. Sep. Purif.*, **9**, 259–270 (1995).

Yun, J.H., D.K. Choi, and S.H. Kim, "Equilibria and Dynamics for Mixed Vapors of BTX in an Activated Carbon Bed," *AIChE J.*, **45**, 751–760 (1999).

Villadsen, J.V. and W.E. Stewart, "Solution of Boundray-Value Problems by Orthogonal Collocation," *Chem. Eng. Sci.*, **22**, 1483–1501 (1967).